CHEMISTRY OF MATERIALS
Article

Chem. Mater. **2010,** *22,* 3511–3518 3511
DOI:10.1021/cm100691a

Assembling Polyoxometalate Clusters into Advanced Nanoarchitectures

Amjad Nisar, Yao Lu, and Xun Wang*

Department of Chemistry, Tsinghua University, Beijing 100084, P. R. China

Received March 8, 2010. Revised Manuscript Received April 22, 2010

We present the polyoxometalate supramolecular nanobuilding blocks-based well-defined and robust rose, snowlike, and ice ball architectures by simple but effective exploitation of noncovalent interactions in the reaction system. All structures begin from the formation of disk assemblies that act as foundation for the construction of diverse, well-defined architectures. The rose, snow flowers, and ice balls, and the corresponding growth mechanisms are unambiguously demonstrated by collecting and analyzing intermediate morphologies. Different assembly shapes show interesting hydrophilic and hydrophobic surface properties which may provide opportunities to develop more suitable functional materials for different systems to overcome the polarity restrictions. All assemblies form through the precisely order and successive organization of polyoxometalate nanosupramolecules in a lamellar pattern that may be prompted or slowed-down by controlling ambient temperature of the reaction system. We expect the well-defined shape and the corresponding nano- and microspacing can act as hosts for foreign gust to develop new multifunctional materials.

Introduction

The exploitation of supramolecular nanobuilding blocks in a controlled engineering mode is a challenging area of growing interest and technological importance to design advanced and well-defined functional materials in chemistry and material science. In this context, a range of materials including block copolymers,[1] aliphatic and aromatic organic compounds,[2] metal ions,[3,4] and biomaterials[5] have been employed to obtain a variety of distinct supramolecular structures with unique physical and chemical properties. In principle, the basic supramolecular building block emerges from the synergistic combination of organic−organic,[2] inorganic−organic,[6] metal−organic,[7] or metal−metal[8] parts, which imparts the essential combinatorial properties to the resulting complex to assemble in the particular shape. The supramolecular self-assemblies can be driven by both covalent and noncovalent interactions. But the noncovalent interactions comprising hydrogen bonding, van der Waals forces, $\pi-\pi$ stacking, charge transfer interactions between electron acceptors and donors, electrostatic interactions, etc., are seeing increased research attention because they impart enhanced versatility, flexibility, reversibility, and dynamic behavior to the consequential assemblies.[9−12] Polyoxometalate (POM) supramolecular clusters, which are intriguing nanosized metal-oxides because of their chemical, structural, and electronic versatility,[13−17] and thus have range of potential applications in numerous fields,[18−22] are the perfect choice for the development of advanced functional materials and devices but have not been yet systematically explored.

Conventional supramolecular nanobuilding blocks can be spontaneously self-assembled to highly defined and controllable structures by manipulating their local nanoenvironment and the thermodynamic equilibrium conditions. In this regards both intra- and intermolecular

*Corresponding author. E-mail: wangxun@mail.tsinghua.edu.cn.

(1) Wang, X.; Guerin, G.; Wang, H.; Wang, Y.; Manners, I.; Winnik, M. A. *Science* **2007**, *317*, 644–647.
(2) Chao, W.; Yinsheng, G.; Yapei, W.; Huaping, X.; Ruji, W.; Xi, Z. *Angew. Chem., Int. Ed.* **2009**, *48*, 8962–8965.
(3) Wang, X.; Zhuang, J.; Peng, Q.; Li, Y. *Nature* **2005**, *437*, 121–124.
(4) Shen, S.; Zhuang, J.; Xu, X.; Nisar, A.; Hu, S.; Wang, X. *Inorg. Chem.* **2009**, *48*, 5117–5128.
(5) Harold, F. M. *Microbiol. Mol. Biol. Rev.* **2005**, *69*, 544–564.
(6) Nisar, A.; Xu, X.; Shen, S.; Hu, S.; Wang, X. *Adv. Funct. Mater.* **2009**, *19*, 860–865.
(7) Li, D.; Zhang, J.; Landskron, K.; Liu, T. *J. Am. Chem. Soc.* **2008**, *130*, 4226–4227.
(8) Xu, X.; Wang, X.; Nisar, A.; Liang, X.; Zhuang, J.; Hu, S.; Zhuang, Y. *Adv. Mater.* **2008**, *20*, 3702–3708.
(9) Percec, V.; Glodde, M.; Bera, T. K.; Miura, Y.; Shiyanovskaya, I.; Singer, K. D.; Balagurusamy, V. S. K.; Heiney, P. A.; Schnell, I.; Rapp, A.; Spiess, H. W.; Hudson, S. D.; Duan, H. *Nature* **2002**, *417*, 384–387.
(10) Lehn, J.-M. *Science* **2002**, *295*, 2400–2403.
(11) Yapei, W.; Huaping, X.; Xi, Z. *Adv. Mater.* **2009**, *21*, 2849–2864.
(12) Meng, L.; Yongge, W.; Bubin, X.; Calida Fung-Chi, C.; Zhonghua, P.; Douglas, R. P. *Angew. Chem., Int. Ed.* **2002**, *41*, 1566–1568.
(13) Miras, H. N.; Cooper, G. J. T.; Long, D.-L.; Bogge, H.; Muller, A.; Streb, C.; Cronin, L. *Science* **2010**, *327*, 72–74.
(14) Müller, A.; Kögerler, P. *Coord. Chem. Rev.* **1999**, *182*, 3–17.
(15) Long, D.-L.; Burkholder, E.; Cronin, L. *Chem. Soc. Rev.* **2007**, *36*, 105–121.
(16) Kortz, U.; Müller, A.; van Slageren, J.; Schnack, J.; Dalal, N. S.; Dressel, M. *Coord. Chem. Rev.* **2009**, *253*, 2315–2327.
(17) Sadakane, M.; Steckhan, E. *Chem. Rev.* **1998**, *98*, 219–238.
(18) Volkmer, D.; Du Chesne, A.; Kurth, D. G.; Schnablegger, H.; Lehmann, P.; Koop, M. J.; Muller, A. *J. Am. Chem. Soc.* **2000**, *122*, 1995–1998.
(19) Zhang, H.; Lin, X.; Yan, Y.; Wu, L. *Chem. Commun.* **2006**, 4575–4577.
(20) Chris, R.; Carsten, S.; Johannes, T.; Scott, G, M.; Haralampos, N, M.; De-Liang, L.; Thomas, B.; Robert, D, P.; Thomas, M.; Leroy, C. *Angew. Chem., Int. Ed.* **2008**, *47*, 6881–6884.
(21) Fleming, C.; Long, D.-L.; McMillan, N.; Johnston, J.; Bovet, N.; Dhanak, V.; Gadegaard, N.; Kogerler, P.; Cronin, L.; Kadodwala, M. *Nature Nanotechnol.* **2008**, *3*, 289–233.
(22) Wei, Q.; Yizhan, W.; Wen, L.; Lixin, W. Chem. Eur. J. **2009**, *9999*, NA.

Published on Web 05/04/2010

noncovalent interactions have been considered and a variety of examples in diverse supramolecular systems have been reported.[11,23,24] Although, there are several reports about the POM self-assemblies but the diversity of the structures is still quite limited. The general instances include Lanmuir−Blodgett films,[25] honeycomb architectures,[26] micelles,[27] onionlike spheres,[6,28] fibers,[29] tubes,[30] and hollow vesicles.[31] Recently, in an effort we developed POM novel disk, cone and tube assemblies.[32] The findings in our previous work urged us to explore POM supramolecular building blocks systematically to construct new assembly shapes of POM, which can fulfill the requirements of different application systems more satisfactorily. Herein, we present POM novel multiple shape flowerlike assemblies which are interesting not only for their shapes but also for their nano and micro spaces and tunable surface properties. To the best of our knowledge, there is no report concerning this kind of complex structures in the field of POM. We expect our effort may provide a new research direction in material science.

Experimental Section

Chemicals. Dimethyldioctadecylammonium bromide (DODA.Br) was purchased from ACROS organics. Phosphotungstic acid ($H_3PW_{12}O_{40}$) and phosphomolybdic acid ($H_3PMo_{12}O_{40}$) were purchased from Sinopharm Chemical Reagent Co. Ltd. (SCRC) while the remaining chemicals used during experimental work were from Beijing Chemical Reagent Industry. All chemicals were of analytical reagent grade and used as received without any further purification.

Synthesis. A single-phase approach[6] was adopted to prepare the SP1 and SP2 supramolecular building blocks. In the particular synthesis of SP1, a weighed amount of $H_3PW_{12}O_{40}$ was added into DODA.Br solution in chloroform so that the initial molar ratio between DODA and $H_3PW_{12}O_{40}$ was kept to 3:1, respectively. The whole content was subjected to ultrasonication until a clear solution was obtained. If there is any turbidity, the solution may be washed with water to get a clear solution and remove any unreacted POM. Finally, the SP1 was collected by evaporation of chloroform. The product was put to be dry at room temperature under vacuum until a constant weight was obtained. Phosphomolybdic acid based supramolecular building block (SP2) was also obtained in the same way. The SPs are immiscible in water, but can readily dissolve in organic solvents such as chloroform, tetrahydrofuran, acetone, or butanone. The POMs supramolecular assemblies including ice ball, snow, and rose flower structures were obtained through optimized solvent systems of acetone, acetone/*n*-butanol, 1-butanone/*n*-butanol, and tetrahydrofuran/*n*-butanol, respectively.

Scheme 1. POM Cluster Combines with Surfactant Cation to forms the POM Supramolecular Nanobuilding Block (SP) That Subsequently Self-Assembles in Specific Nanoenvironment to Produce Rose Flowers (RF), Snow Flowers (SF), and Ice Balls (IB)

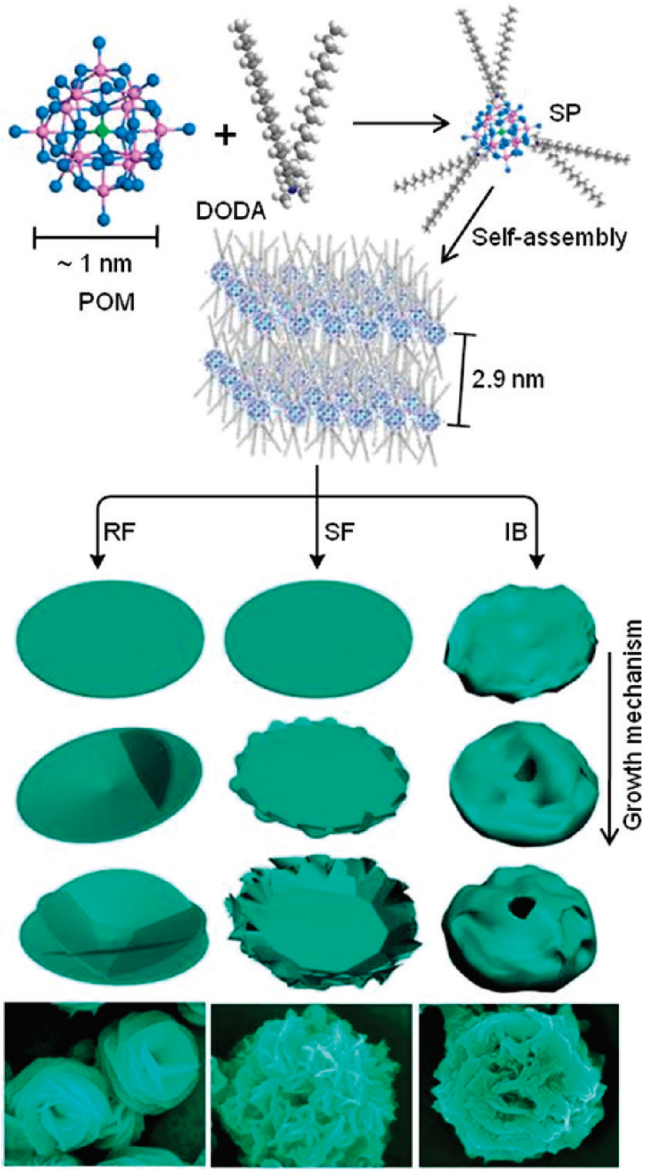

Characterization. The morphologies and structural details of the POM supramolecular assemblies were studied by JEOL JEM-1200EX and FEI Tecnai G2 F20 S-Twin transmission electron microscopes (TEM), whereas TEM samples were prepared on carbon coated copper grid by a dip coating technique. Scanning electron microscopy (SEM) investigations were performed on FEI Sirion 200 scanning electron microscope by depositing sample on a silicon wafer. Fourier transform infrared spectrometry measurements were performed on Nicolet AVATAR 360 ESP FTIR using KBr pellet. The ^{1}HNMR spectra were obtained by JEOL ECA-600 NMR spectrometer. Thermogravimetric analysis was carried out under a N_2 atmosphere, with a heating rate of 10 °C/min by TA Instruments Q5000 IR thermogravimetric analyzer (TGA). The Elemental analysis was performed on EAI CE-440 elemental analyzer. The small angle

(23) Takashi, N.; Katsuhiko, A.; Tsuyoshi, M.; Kaname, Y.; Hirokazu, T.; Toshiharu, T.; Helmuth, M.; Dirk, G. K. *Small* **2007**, *3*, 2019–2023.
(24) Hu, S.; Wang, X. *J. Am. Chem. Soc.* **2008**, *130*, 8126–8127.
(25) Bao, Y.-Y.; Bi, L.-H.; Wu, L.-X.; Mal, S. S.; Kortz, U. *Langmuir* **2009**, *25*, 13000–13006.
(26) Fan, D.; Jia, X.; Tang, P.; Hao, J.; Liu, T. *Angew. Chem., Int. Ed.* **2007**, *46*, 3342–3345.
(27) Weifeng, B.; Sayaka, U.; Noritaka, M. *Angew. Chem., Int. Ed.* **2009**, *48*, 8281–8284.
(28) Li, H.; Sun, H.; Qi, W.; Xu, M.; Wu, L. *Angew. Chem., Int. Ed.* **2007**, *46*, 1300–1303.
(29) Carraro, M.; Sartorel, A.; Scorrano, G.; Maccato, C.; Dickman, M. H.; Kortz, U.; Bonchio, M. *Angew. Chem., Int. Ed.* **2008**, *47*, 7275–7279.
(30) Ritchie, C.; Cooper, G. J. T.; Song, Y.-F.; Streb, C.; Yin, H.; Parenty, A. D. C.; MacLaren, D. A.; Cronin, L. *Nat. Chem.* **2009**, *1*, 47–52.
(31) Liu, T.; Diemann, E.; Li, H.; Dress, A. W. M.; Muller, A. *Nature* **2003**, *426*, 59–62.
(32) Nisar, A.; Zhuang, J.; Wang, X. *Chem. Mater.* **2009**, *21*, 3745–3751.

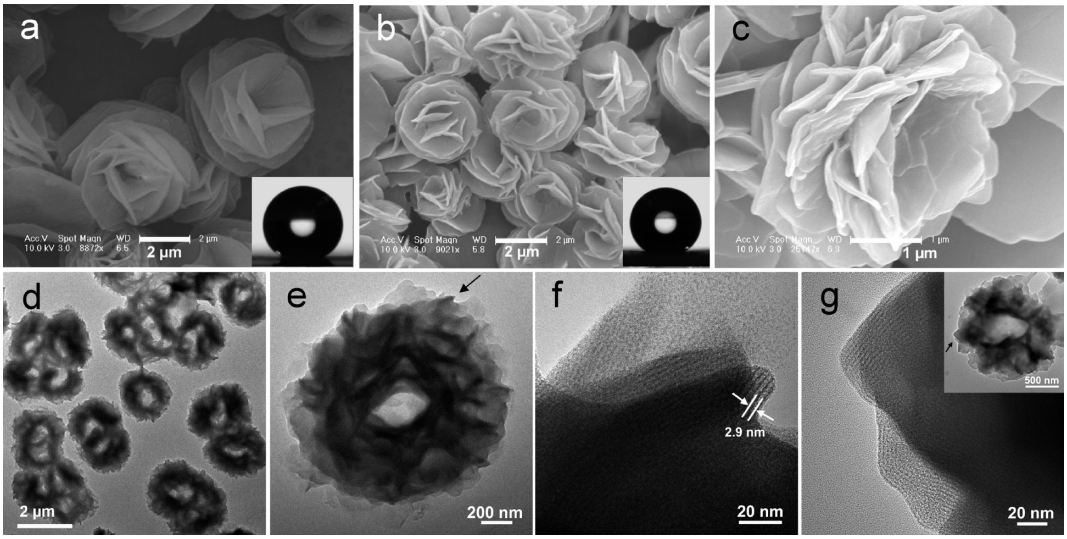

Figure 1. POM rose flowers. (a) SEM image of SP1 rose flowers. (b) SEM image of SP2 rose flowers. The insets show the static contact angle of a film of the assemblies (146 and 151°, respectively). (c) SEM image of a SP1 rose-flower at different angle. (d) TEM image of SP1 rose flowers. (e) Magnified TEM image of a SP1 rose-flower. (f) HRTEM image of the part of the flower mentioned in part e. (g) HRTEM image of the part of the SP2 rose flower mentioned in the inset.

X-ray diffraction patterns of the dried powdered samples of particular shapes were obtained by Rigaku D/max-2500/PC X-ray diffractometer using CuKα radiation ($\lambda = 1.5418$ Å). Water drop static contact angle assessments were made at room temperature using OCA 20, DataPhysics Instruments GmbH, Filderstadt, Germany, by sessile drop and tilting plate measuring method.

Results and Discussion

Phosphotungstic and phosphomolybdic acids serve as the backbone of POM chemistry. Inspired by these two basic POMs a huge class of inorganic compounds of varying structures and chemical natures is constructed. The POM supramolecular building blocks $(DODA)_3PW_{12}O_{40}$, SP1, and $(DODA)_3PMo_{12}O_{40}$, SP2, were prepared using previously described the single-phase approach (DODA = dimethyldioctadecylammonium).[6] Both SP1 and SP2 were characterized by Fourier transform infrared spectrometry, ^{1}HNMR spectroscopy, thermogravimetric analysis, elemental measurements, and X-ray energy-dispersive spectroscopy (see the Supporting Information). The FTIR spectra show the characteristics band of both DODA and POM. Elemental analysis and weight fractions measurements indicate the respective formulas of SP1 and SP2. Further, the ^{1}HNMR measurements of SP1 and SP2 demonstrate the POM and organic surfactant supramolecular complex formation through columbic forces in terms of broadening and shifts of resonance signals of *N*-methyl and *N*-methylene protons to upfield.

The electrostatic interactions between POM and organic surfactant are of high significance and dynamic applications, and by exploiting these noncovalent interactions, POM can be manipulated in different ways to develop new functional materials. The schematic diagram in Scheme 1 shows the POM rose, snow flower, and ice ball assemblies that we have achieved by controlling and manipulating the local nanoenvironment of the SP1and SP2.

Rose Flowers. Roselike structures of POM were obtained from the optimized mixed solvent of tetrahydrofuran and *n*-butanol in a 3:1 volumetric ratio. Figure 1a−c and Figure S7 in the Supporting Information show the scanning electron microscopy (SEM) images of the rose flowers obtained from SP1 and SP2. High-magnification images at different angles demonstrate how POM orderly self-organize into petals to generate rose-like flower architecture (Figure 1c and Figure S7 in the Supporting Information). Transmission electron microscopy (TEM) images further demonstrate the similarity between the POM flower and the natural flower. Figure 1d shows a clear contrast between the sepal-central and petal-outer parts. The observation of magnified image reveals that the central part is quite thin, whereas the outer part is thick because it has a number of petal layers (Figure 1e and Figure S8 in the Supporting Information). The high-resolution image of the edges shows that the flowers are composed of multilamellar nanostructures (Figure 1f,g), which demonstrate that under particular surrounding interactions SP1 and SP2 self-assemble in well-defined and organized patterns (Figure1). Interestingly, TEM and SEM investigations of SP1 and SP2 samples obtained from pure tetrahydrofuran did not reveal any assembly shape, whereas the addition of *n*-butanol in optimized ratio results in very stable and well-defined roselike flowers.

Snow Flowers. In our experimentation, the shape of the assembly structures was found to be highly dependent to the local environment of the SP1 and SP2. To further explore the SP1 and SP2 assembly behavior, we tried to develop POM assembly structures in different solvent systems. Figure 2 shows the SEM and TEM images of snowlike spherical flowers obtained from the self-assembly of SP1 and SP2 in acetone/*n*-butanol (3:1 v/v) mixed solvent. Both TEM and SEM images indicate that the assemblies are composed of dozens of petals that randomly combine with each other to create snowlike flower shape. Interestingly, the assemblies were found to have narrow hole along the diagonal in the center. The high-resolution TEM images show the similar lamellar morphology to the rose structures (Figure 2g,j).

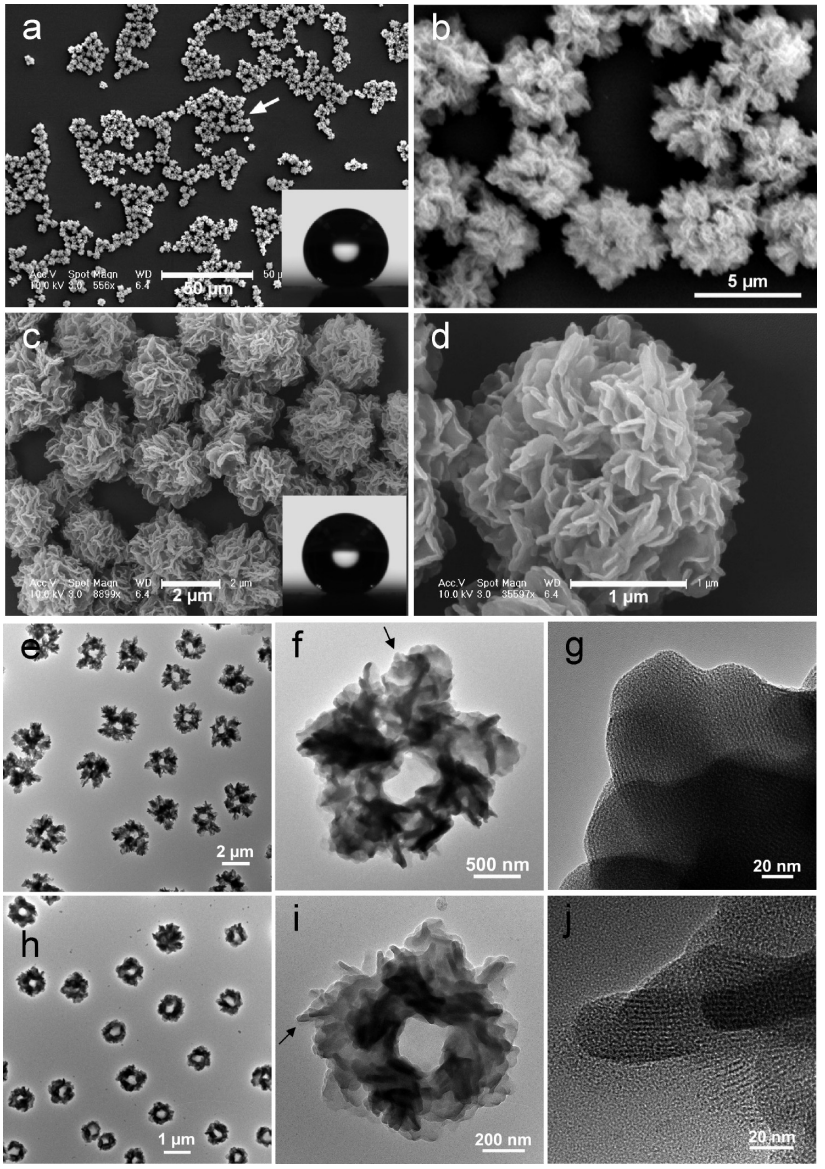

Figure 2. POM snow flowers. (a) SEM image of SP1 snow-flowers. (b) Magnified SEM image of the region indicated in part a. (c) SEM image of SP2 snow flower. (d) Magnified SEM image of a SP2 snow flower. (e, f) TEM image of a SP1 snow flowers indicating the hollow interior. (g) HRTEM image of the edge of the flower mentioned in part f. (h, i) TEM image of SP2 snow flowers indicating the hollow interior. (j) HRTEM image of the edge of the flower mentioned in part i. The insets in parts a and b show the static contact angle of the films of the corresponding assemblies (157 and 156°, respectively).

Ice Balls. Contrary to the pure tetrahydrofuran solution system, stable assemblies of SP1 and SP2 were also found from the pure acetone solution, which may be owed to the relatively moderate polarity of acetone compared to tetrahydrofuran. Figure 3 and Figure S9 in the Supporting Information demonstrate the POM assemblies obtained from the acetone solution. The TEM images illustrate that the assemblies have a similar continuous hole in the center but exhibit more dark and dense outer part (Figure 3c,g). Magnified SEM images (Figure 3b,f) further clarify the TEM observations and demonstrate that although assemblies are similar to snow flowers but exhibit relatively aggregated and more dense surface morphology. Further, detailed scanning by high-resolution TEM reveals a mixed, layered, and tiny-particle-nature morphology (Figure 4d,h and Figure S12 in the Supporting Information).

XRD Measurements. Small-angle XRD analyses of the different flower assemblies of both SP1 and SP2 show a feature typical of layered structures. The characteristic first-, second-, and third-order reflection peaks correspond to interlayer spacing of about 2.9 nm for both SP1 and SP2, respectively, and support well the high-resolution TEM results of lamellar nature (Figure 4a and the Supporting Information, Figure S13). The similarity of interlayer spacing may be attributed to the equivalent ionic size of SP1 and SP2. However, particularly for SP2 ice balls, we observed an additional diffraction peak of about 3.5 nm interlayer spacing, which interestingly almost completely disappears with the addition of *n*-butanol in the reaction system. As pure DODA.Br exhibits the interlayer spacing of about 3.6 nm (see the Supporting Information, Figure S14), so we speculate the appearance of 3.5 nm peak in XRD pattern is due to relative loss packing of DODA alkyl chains in the ice balls, which results in similar behavior as in pure DODA. Furthermore, wide-angle XRD patterns confirm the conformational order of the surfactant in the

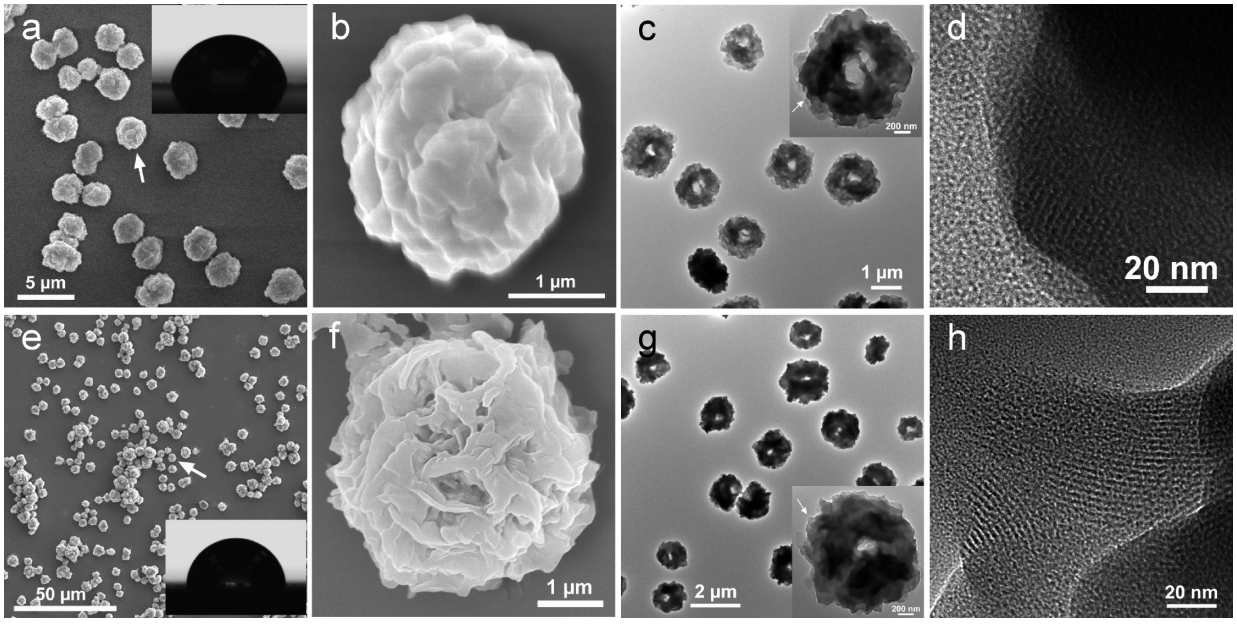

Figure 3. POM ice balls. (a) SEM image of SP1 ice balls. (b) Magnified SEM image of the ice ball mentioned in part a. (c) TEM image of SP1 ice balls indicating the hollow interior. (d) HRTEM image of the edge of an ice ball indicated in part c. (e) SEM image of SP2 ice balls. (f) Magnified SEM image of a SP2 ice ball illustrating the surface morphology. (g) TEM image of SP2 ice balls. (h) HRTEM image of the edge of an ice ball mentioned in part g. The insets in parts a and e show the static contact angle of the films of the corresponding assemblies (~81 and ~89°, respectively).

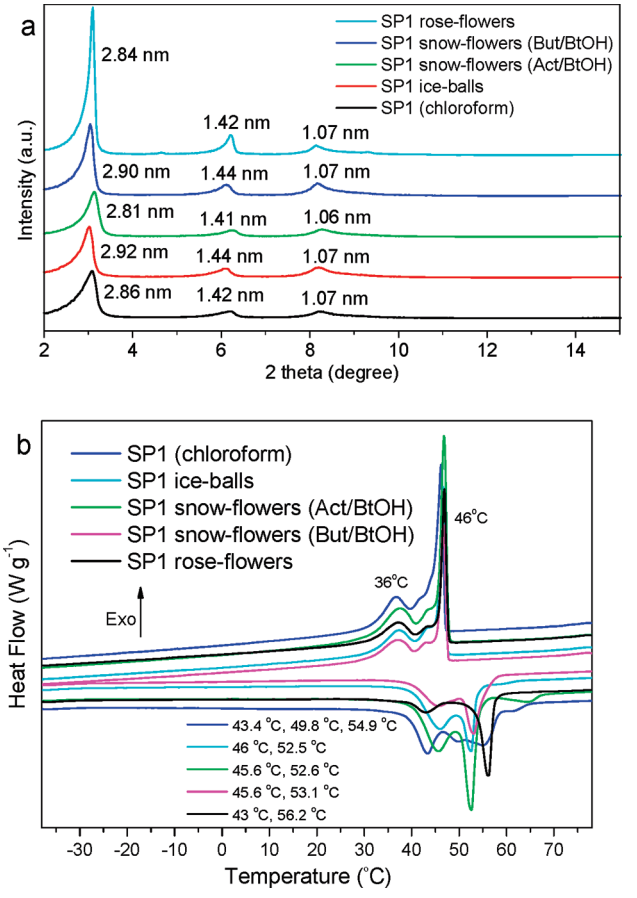

Figure 4. (a) Powder XRD patterns of SP1 assembly structures in low-angle region demonstrating the presence of lamellar morphology with only one type of layer spacing. (b) DSC curves of SP1 dried assemblies in heating−cooling cycle at scanning rate of 5 °C/min. Act/BtOH = acetone/*n*-butanol and But/BtOH = butanone/*n*-butanol.

supramolecule and show reflection peaks of about 0.42 nm, which agrees well with the lateral packing of alkyl chains and indicates their close packing in the POM assembly structures (see the Supporting Information, Figure S15 and S16).[33,34]

Static Contact Angle Measurements. As indicated by TEM and SEM analysis although ice balls and snow flowers have similar spherical shape but their assembly structures are quite different. To understand the surface properties of the different assemblies, we performed static contact angle measurements of smooth film of the assemblies. The large static contact angle of about 150° of rose and snow flowers (Figures 1a,b and 2a,c) indicates that the assemblies have superhydrophobic surface properties, which indicates that in assemblies POMs are fully surrounded by DODA alkyl chains and closely packed to protect hydrophilic POMs from the hydrophobic solvent environment. Interestingly, the static contact angle for ice balls was estimated to be less than 90° (Figure 3a,e), which suggests that POMs in the assemblies are not completely surrounded by DODA alkyl chains and moderately hydrophilic in nature. Further, formation of stable dispersion in water also supports the contact angle measurements.

Phase Transition Studies. To further explore the POM supramolecular building blocks and their assembly mechanism in different nanoenvironments, the thermal behavior of the assemblies in both the solution and solution-free dried states was studied. Typically, lamellar structures made of synthetic surfactants exhibits a phase transition of alkyl chains during the heating and cooling process. In this regard, a variety of structures composed of merely surfactants and even complex hybrid systems have been reported.[28,35,36]

(33) Okuyama, K.; Soboi, Y.; Iijima, N.; Hirabayashi, K.; Kunitake, T.; Kajiyama, T. *Bull. Chem. Soc. Jpn.* **1988**, *61*, 1485–1490.
(34) Bu, W.; Wu, L.; Hou, X.; Fan, H.; Hu, C.; Zhang, X. *J. Colloid Interface Sci.* **2002**, *251*, 120–124.
(35) Blandamer, M. J.; Briggs, B.; Cullis, P. M.; Engberts, J. B. F. N. *Chem. Soc. Rev.* **1995**, *24*, 251–257.
(36) Fendler, J. H. *Acc. Chem. Res.* **1980**, *13*, 7–13.

Differential scanning calorimetric (DSC) analysis of SP1 in chloroform and acetone shows endothermic transition at about 8.4 and 7.8 °C with enthalpy change of about 34.1 and 33.68 kJ/mol in heating process and at about −7.3 and −7.4 °C in the cooling process with similar enthalpy change, respectively (see Figure S17 in the Supporting Information). The calculated enthalpy change is consistent with the already-reported studies.[37,38] Surprisingly, no transition peak was found from −40 to 40 °C for SP1 in acetone/*n*-butanol solution. The disappearance of the phase transition peak with the addition of *n*-butanol in acetone solvent may be attributable to the enhanced rigidity and more stiffed packing of the DODA alkyl chains because of an increase in solvent polarity and thus corresponding hydrophobic interactions. Figure 4b shows the DSC results of the SP1 assemblies in the solvent-free dried state. All assembly structures show a broad peak with mainly two maxima both in heating and cooling process.[39] With little variations the ice balls and snow flowers show endothermic maxima at about 46 and 53 °C with enthalpy change of about 34 kJ/mol. The rose-flowers reveal endothermic maxima at 43 and 56 °C with an enthalpy change of about 28 kJ/mol, which may be attributed to the quite different assembly shapes of the ice-balls and snow-flowers. Interestingly, the phase transition enthalpy change (~34 kJ/mol) of the solvent-free assemblies is equivalent to the assemblies in chloroform and acetone solutions. These results suggest that DODA alkyl chains and the corresponding POM supramolecular building block exhibit similar assembly behavior both in the solution and solution-free dried states.

^{1}H NMR spectroscopy is another valuable technique to study the thermotropic behavior and mobility of alky chains of organic surfactants in hybrid materials.[28,40] Figure S18 (see the Supporting Information) and Figure 5a show the temperature-dependent ^{1}HNMR spectra of the SP1 in $CDCl_3$ and CD_6CO from −40 to 40 °C in the cooling and heating process. It can be seen that at lower temperatures, the proton signal are quite weak and rise slowly, but when temperature approaches the phase transition temperature, a rapid increase occurs and characteristic *N*-methyl and *N*-methylene protons signals of SP1 become clear. These results demonstrate that below transition temperature, the DODA alkyl chains of SP1 are stiffly packed and are in instructed gel crystalline state because of strong hydrophobic interactions but at phase transition temperature become more mobile and transfer to relaxed liquid crystalline state. The similar behavior of phase transition was also found for SP1 in acetone solution and SP2 in $CDCl_3$ solution (Figure 5b and the Supporting Information, Figure S19).

Assembly Mechanism. To investigate the assembly mechanism we collected the starting and intermediate

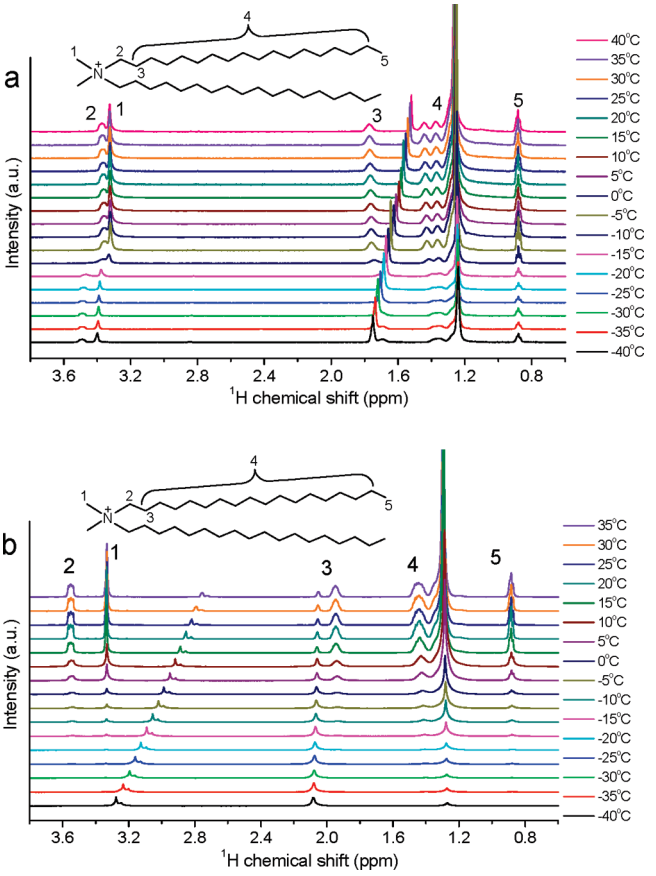

Figure 5. (a) SP1 temperature-dependent ^{1}HNMR spectra in $CDCl_3$ during cooling process. (b) SP1 temperature-dependent ^{1}HNMR spectra in CD_6CO during the heating process.

morphologies at different time intervals. It was found that POM supramolecules immediately form the fine circular disks in the reaction system, which subsequently act as foundation for the growth of the rose structures (Scheme 1 and Figure S20 in the Supporting Information). Figure 6a−d shows the different intermediate stages of rose structure growth. The SEM images clearly demonstrate the assembly process in term of successively increasing number of petal layers on the disk surface which eventually form a roselike structure with multiple layers of petals and a hollow interior. Similar to the rose assemblies, snowlike assemblies also grow from disk assemblies but exhibit different mechanism of growth. In case of snow flowers initially small petals emerge near the periphery of disk which subsequent become bigger and bigger with simultaneously emergence of new petals on the surface of the disk. From Figure 6e−h and Figure S21 in the Supporting Information, it is interesting to note that the growth occurs from the periphery toward the center with continuous reduction of the smooth surface interior and eventually results in a spherical flower with a narrow hole in the center (Figure 2b,d,). Ice balls were also found to be grown from disks having uneven shape and the corresponding growth was found to be in the form of random self-assembly of POM building blocks without any petallike structure formation (see the Supporting Information, Figure S22).

Temperature-Dependent Assembly Behavior. Furthermore, in our experimentation, particularly for rose flowers,

(37) Takashi, N.; Makoto, M.; Hiroto, M.; Takamasa, S.; Naotoshi, N. *Chem.—Eur. J.* **2002**, *8*, 1641–1648.
(38) Feitosa, E.; Bonassi, N. M.; Loh, W. *Langmuir* **2006**, *22*, 4512–4517.
(39) Cocquyt, J.; Olsson, U.; Olofsson, G.; Meeren, P. V. d. *Colloid Polym. Sci.* **2005**, 283.
(40) Ru, G.; Wang, N.; Huang, S.; Feng, J. *Macromolecules* **2009**, *42*, 2074–2078.

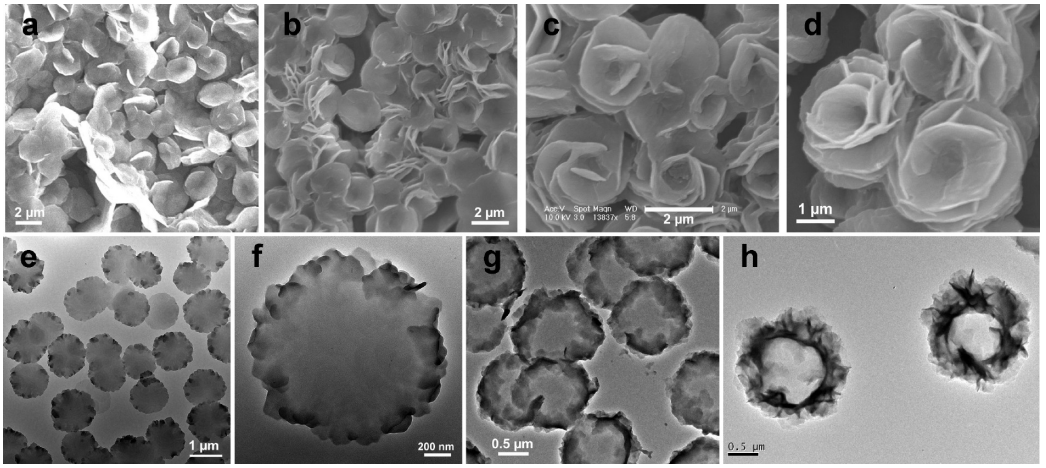

Figure 6. Growth mechanism of POM architectures. (a) SEM image of SP1 rose flowers in initial stage−disks mostly with only one petal (2 min). (b) SEM image of SP1 rose flowers with few number of petals (15 min). (c, d) Rose flowers with successively increasing number of petals and resulting shape evolution (60 min, 90 min, respectively). (e) TEM image of SP2 snow flowers with in initial stage−disks with small petals emerging from the periphery (1 min). (f) Magnified TEM image of one of disk. (g, h) TEM images of the SP2 snow flowers intermediate stages demonstrating successive growth from disk to snow flower with narrow hole in center (5 and 10 min, respectively).

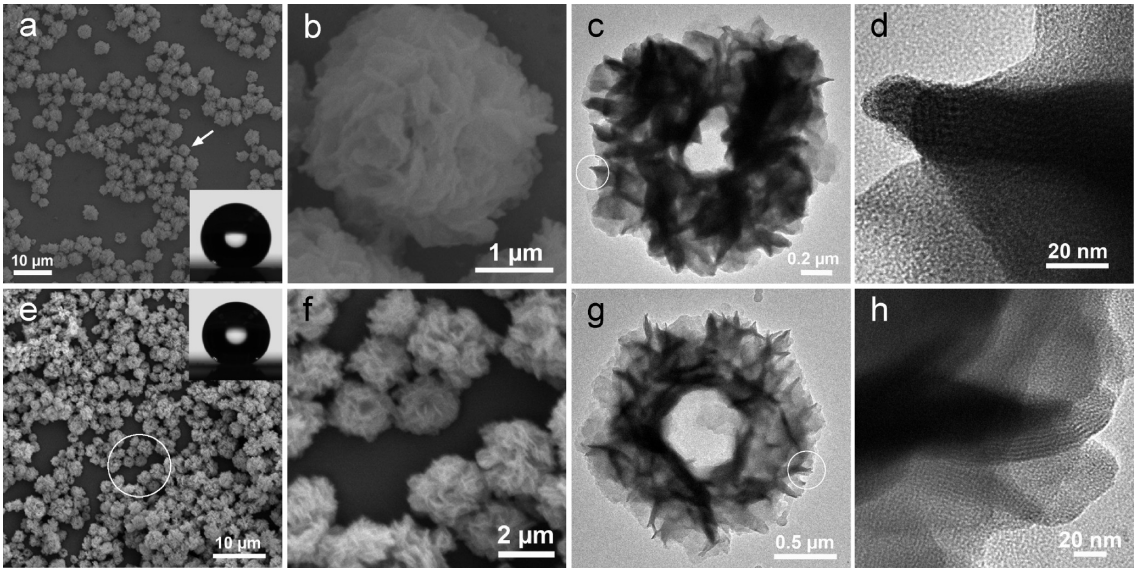

Figure 7. POM snow flowers from butanone/butanol system. (a,b) SEM images of SP1 snow flowers. (c) TEM image of a SP1 snow-flower. (d) HRTEM image of the part of flower mentioned in part c. (e,) SEM images of SP2 snow-flowers. (g) TEM image of a SP2 snow flower. (h) HRTEM image of the edge of the flower mentioned in part g. The insets in parts a and b show the static contact angle of the films of the corresponding assemblies (∼154 and ∼156°, respectively).

the assembly speed was found to depend on the ambient temperature. During a series of experiments, it was observed that at lower temperature (< 15 °C) POM supramolecules assemble quite rapidly and form mature flower structures within 02 h with high purity, whereas at higher temperature (> 30 °C), it becomes considerably slow and may rise up to 1 week. Snow flower assemblies was also found to show similar behavior. At lower temperature (< 15 °C) fully grown assemblies were obtained within 20 min, whereas at higher temperature, assembly time may rise up to 24 h. The slow assembly speed may be due to the predominantly elevated thermal motion of the surfactant's alkyl chains at higher temperature, which eventually disturbs the thermodynamic equilibrium between different noncovalent interactions in reaction system and shifts toward disks assemblies. In addition, DSC and temperature-dependent ^{1}HNMR spectroscopy studies support this conclusion.

The different assembly shapes and varying growth mechanisms may be attributed to the different solvent natures and thus varying noncovalent interactions. All assembly structures are highly stable, and their size, shape, and chemical nature show no change over a period of several months. In an extension of our work, we found that a similar snowlike structure can also be obtained using butanone/*n*-butanol solvent system having similar lamellar morphology and superhydrophobic surface properties (Figure 7).

Conclusions

In summary, we have presented the POM-based structurally well-defined rose- and snow- flower-, and ice-ball-like

architectures by simply exploiting noncovalent interactions including electrostatic, dipole−dipole, van der Waals, hydrogen bonding, solvophobic interactions, and hydrophobic interactions between the POM supramolecules. In addition, the specific number of surfactant's molecules attached with POM cluster also plays a significant role to develop assembly structure of particular shape. Interestingly, all flower assemblies route through the formation of the disks, which subsequently serve as foundation for development of whole structure. The nanospacing due to lamellar nature of assemblies and microspaces between petals may serve as hosts for nano- and microsized guests, which may help to develop multifunctional composite materials for applications like catalysis and energy storage. Further varying hydrophilic and hydrophobic surface properties of different structures may provide additional opportunity to design suitable functional materials for different polarity systems. In further work, we aim to utilize these assemblies for different applications like catalysis and medicine.

Acknowledgment. This work was supported by NSFC (20725102, 50772056), the Foundation for the Author of National Excellent Doctoral Dissertation of P. R. China, the Program for New Century Excellent Talents of the Chinese Ministry of Education, the Fok Ying Tung Education Foundation (111012), and the State Key Project of Fundamental Research for Nanoscience and Nanotechnology (2006CB932301).

Supporting Information Available: FTIR spectra of POM supramolecules (SP1 and SP2) and their assembly structures, elemental analysis, TGA analysis, energy-dispersive spectroscopy (EDS) spectra, small- and wide-angle XRD patterns, DSC curves of SP1 in chloroform and acetone, temperature-dependent 1HNMR spectra, and SEM and TEM images of rose flowers, snow flowers, and ice balls (PDF). This material is available free of charge via the Internet at http://pubs.acs.org.